doi:10.1246/cl.2010.334

Synthesis of Ag@Cu Core–Shell Nanoparticles in High Yield Using a Polyol Method

Masaharu Tsuji,*[1,2,3] Sachie Hikino,[1] Ryuichi Tanabe,[2] and Daiki Yamaguchi[3]
[1]*Institute for Materials Chemistry and Engineering, Kyushu University, Kasuga 816-8580*
[2]*Department of Energy Science and Engineering, Faculty of Engineering, Kyushu University, Kasuga 816-8580*
[3]*Department of Applied Science for Electronics and Materials, Graduate School of Engineering Sciences, Kyushu University, Kasuga 816-8580*

(Received December 28, 2009; CL-091159; E-mail: tsuji@cm.kyushu-u.ac.jp)

Ag core–Cu shell nanoparticles, denoted as Ag@Cu, were synthesized in high yield (100%) using a one-pot polyol method under bubbling Ar gas. $AgNO_3$ and $Cu(OAc)_2{\cdot}H_2O$ were used as reagents. The formation of Ag@Cu particles and their crystal structures were examined using energy dispersed X-ray spectroscopic (EDS) measurements and selected area electron diffraction (SAED) patterns. The growth mechanism of Ag@Cu is discussed.

Bimetallic nanoparticles have excellent optical, electronic, and catalytic properties different from those of the component metals. Therefore, much attention has been received for the development of novel synthesis methods for bimetallic nanoparticles and their applications as catalysts, sensors, and substrates for surface-enhanced Raman scattering.[1–4] We have recently initiated shape-, size-, and composite-controlled syntheses of Ag/Cu bimetallic nanoparticles. In our previous studies, we prepared Ag/Cu bimetallic nanoparticles such as Cu@Ag core–shell and Cu/Ag phase-separated bicompartment by a polyol method.[5,6]

Ag@Cu core–shell particles are also interesting Ag/Cu bimetallic particles for both fundamental and technological purposes. Cazayous et al.[7] obtained Ag@Cu particles in high yield by thermal evaporation of Ag and Cu under ultrahigh vacuum. Since an ultrahigh system is necessary in this method, a more simple low-cost method is required for mass production of Ag@Cu. Nakamura et al.[8] prepared Ag@Cu particles using two-step microwave-assisted alcohol reduction. Although this method is a simple low-cost technique for mass production of Ag@Cu in solution, their maximum yield was only 17%. The low yield of Ag@Cu particles prevented measurements of their intrinsic optical and chemical properties and practical application of this technique.

In the present study, we attempted to develop a new simple one-pot preparation method of Ag@Cu particles using a polyol method. We succeeded in the preparation of Ag@Cu particles in high yield (100%). The crystal structure and the growth mechanism of Ag@Cu particles are discussed on the basis of transmission electron microscopic (TEM)–EDS data and SAED patterns.

At first we attempted to synthesize Ag@Cu particles by reducing $AgNO_3$ in ethylene glycol (EG) in two steps. Initially Ag cores particles were prepared from $AgNO_3$, and then $Cu(OAc)_2{\cdot}H_2O$ was added for the preparation Cu shells. However, no Cu@Ag core–shell particles were obtained, and the products were Cu/Ag bicompartmental particles.[6] Thus, in this work we attempted to prepare Ag@Cu particles by changing experimental procedures and parameters such as reaction temperature and heating time. We then found that the reverse addition of the two reagents was preferred for the preparation of Ag@Cu particles. At first 8 mL of 15.9 mM $Cu(OAc)_2{\cdot}H_2O$ in EG and 8 mL of 477 mM poly(vinylpyrrolidone) (PVP, MW: 55000 in terms of monomer units) in EG were mixed in a 100-mL three-necked flask, and Ar was bubbled at room temperature for 10 min to remove oxygen dissolved in the solution. It was soaked in an oil bath preheated at 180 °C. Then the solution was rapidly heated from room temperature to 175 °C over a few minutes under bubbling Ar. Then 2 mL of 15.7 mM $AgNO_3$ was added and the reagent solution was maintained at 175 °C for 20 min under bubbling Ar. The final concentrations of $Cu(OAc)_2{\cdot}H_2O$, $AgNO_3$, and PVP were 7.0, 1.7, and 212 mM, respectively. The reagent solution was sampled at various reaction times to examine the formation mechanism of Ag@Cu.

Product solutions were centrifuged at 13000 rpm three times for 15 min each time. The precipitates were collected and then redispersed in deionized water. For TEM (JEM-2100XS and 2100F; JEOL) observations, samples were prepared by dropping colloidal solutions of the products onto Au grids. Absorption spectra of the product solutions were measured using a spectrometer (UV-3600; Shimadzu Corp.) in the UV–visible (vis) region.

Figures 1a–1d and 1e–1h depict typical TEM images, and their EDS data of product particles obtained after addition of $AgNO_3$ and keeping reagent solution at 175 °C for 5 and 20 min, respectively. Although distinguishing between Cu and Ag from the contrast of TEM images depicted in Figure 1a is difficult, EDS data shown in Figures 1b–1d show that Ag@Cu particles were prepared in high yield (100%).

Figure 2a portrays distributions of the Ag and Cu components along the cross section line of a typical particle shown in Figure 1d. These line analysis data for several particles implied that ca. 5-nm Cu shells were overgrown on spherical Ag cores with an average diameter of 94 ± 28 nm.

Although some TEM images obtained after heating for 20 min (Figure 1e) show dark and bright contrast due to Ag cores and Cu shells, respectively, no definite conclusion can be obtained for all products from contrast of images. EDS data shown in Figures 1f–1h clearly indicate that Ag@Cu particles (104 ± 23 nm) with thicker Cu shells are prepared in high yield (100%). Figure 2b shows the line analysis data of Ag and Cu components along the cross section line for a typical Ag@Cu particle shown in Figure 1h. On the basis of the EDS data and their line analyses, it was found that ca. 20-nm Cu shells are overgrown on Ag core particles. The atomic ratios of Ag:Cu at 5 and 20 min were determined to be 85:15 and 31:69, respectively, indicating that Cu component increased with increasing heating time. Many vacancies observed in Figures 1d and 1h indicate

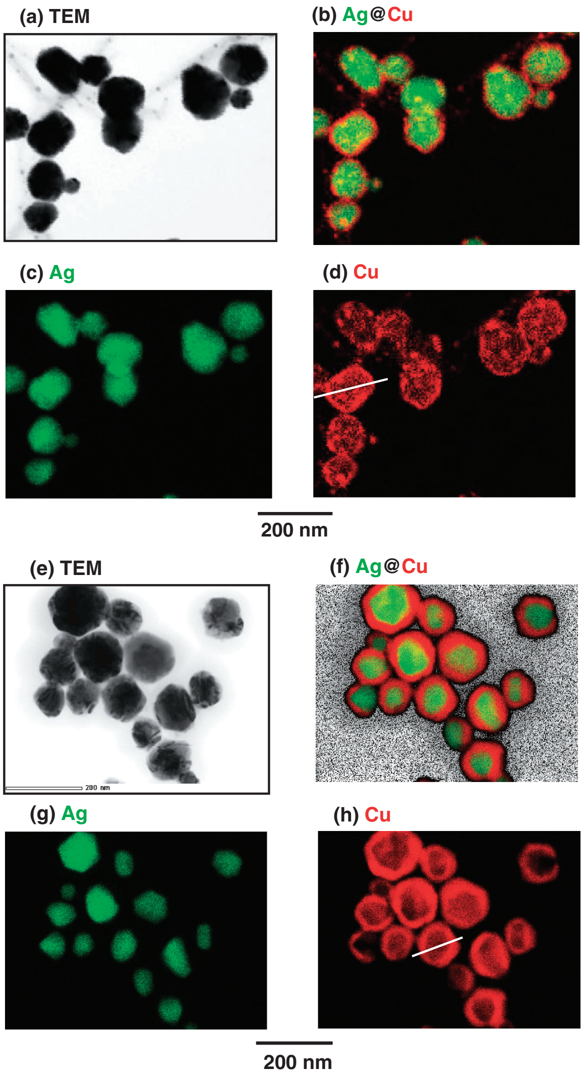

Figure 1. TEM images and their EDS data of Ag@Cu nanoparticles: (a)–(d): after heating for 5 min and (e)–(h): after heating for 20 min.

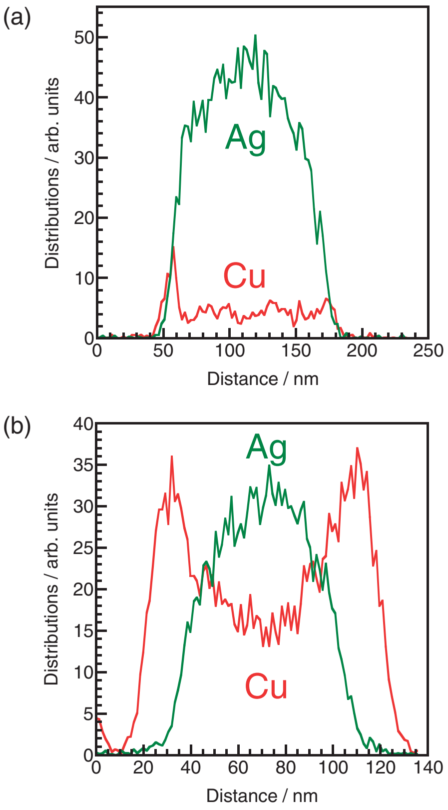

Figure 2. Distributions of Ag and Cu components in typical Ag@Cu particles along lines shown in Figure 1. (a) After heating for 5 min and (b) after heating for 20 min.

that no Ag/Cu alloy cores are incorporated into the particles in place of the Ag core.

Figures 3a and 3b show the TEM image and the SAED pattern of a typical Ag@Cu particle. We could observe many ED spots of (111), (200), and (220) facets and some other facets of Ag and Cu in SAED patterns. On the basis of these findings, it was concluded that Ag@Cu particles are not amorphous but polycrystals having a fcc type of crystal structure.

Figure 4a shows color change of the product solution. Just after injection of $AgNO_3$, the solution color starts to change and after heating for 2 min a light green solution was obtained. It changes from brown into red with increasing heating time from 5 to 20 min. These changes suggest that optical properties change from silver to copper with increasing heating time.

The UV–vis spectra were measured to characterize optical properties and to examine time evolution of crystal growth of Ag@Cu particles (Figure 4b). For comparison UV–vis spectra of $Cu(OAc)_2 \cdot H_2O$ and typical spherical Ag and Cu particles in EG are also shown. Little absorption exists >400 nm for $Cu(OAc)_2 \cdot H_2O$, whereas spherical Ag and Cu particles give surface plasmon resonance (SPR) bands with peaks at ca. 400 and ca. 600 nm, respectively. Before the addition of $AgNO_3$, no SPR peak of Cu particles was observed, indicating that there were no Cu nanoparticles formed in the solution. By the addition of $AgNO_3$, solution color rapidly changed, and after heating for 2 min at 175 °C, a broad SPR band with a peak at 460 nm was observed. With increasing heating time from 2 to 8 min, the intensity of the SPR band increased, and the SPR band shifted from 460 to 550 nm. After heating for 12 min, an SPR band with a peak at ca. 600 nm was observed. In the 12–20 min range, no significant peak shift and change in intensity were observed. These spectral changes indicate that Ag is the main component of the product particles in the initial stage. With increasing heating time, SPR band of Cu shell component increased, and the formation of Ag@Cu particles completed at about 12 min. The SPR band of Ag component at 400 nm slightly decreased in the 12–20 min range. UV–vis, and TEM–EDS data shows that the thickness of Cu shells can be controlled by changing the heating time in the 2–12 min range.

On the basis of TEM–EDS and UV–vis spectral data at various reaction stages, it is reasonable to assume that Ag@Cu is grown through the following mechanism. Since the standard potential of Cu^{2+}/Cu^0 (+0.34 eV) is relatively low, the reduction rate of Cu^{2+} is slow. Therefore, few Cu particles were formed before the addition of $AgNO_3$ at 175 °C. On the other hand, since the standard potential of Ag^+/Ag^0 (+0.78 eV) is relatively high, the reduction rate of Ag^+ is fast. Therefore, Ag^+ is reduced to

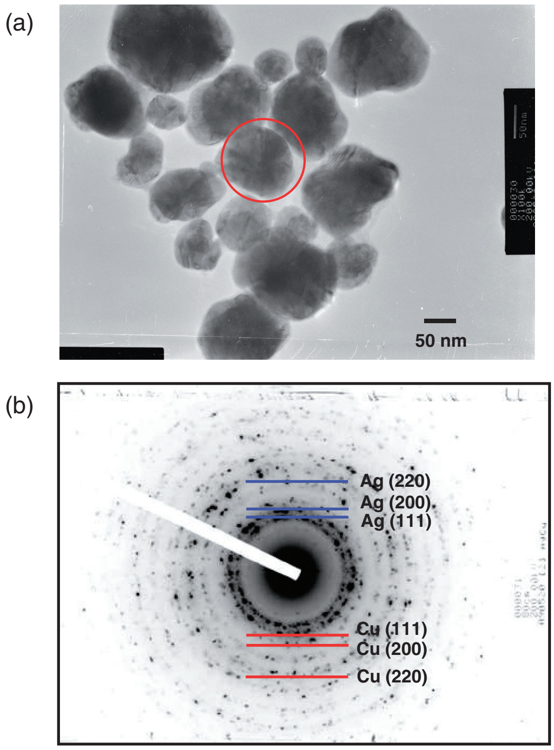

Figure 3. (a) TEM and (b) SEAD pattern of Ag@Cu particles surrounded by a red circle in (a).

Ag^0 rapidly after addition of $AgNO_3$. It should be noted that the reduction of Cu^{2+} is strongly enhanced by the addition of $AgNO_3$. In order to clarify whether Ag^+ or Ag seeded particles are responsible for this effect, we added Ag nanoparticles to $Cu(OAc)_2 \cdot H_2O$/PVP/EG solution at 175 °C.[9] As a result, the reduction of Cu^{2+} was also enhanced, indicating that Ag nanoparticles took part in the enhancement of the reduction of Cu^{2+}.

A similar enhancement of reduction of Sn^{2+} in the presence of gold has been observed.[10] This effect was explained by the cathodic polarization of the Au particles by electron transfer from organic radicals generated in the radiolysis and subsequent reduction of Sn^{2+} directly on the surface of the Au particles. A similar cathodic polarization of Ag nanoparticles may occur in the polyol reduction, where some organic radicals and electrons are formed as intermediates in the thermal decomposition of EG.[11]

$$CH_2OH\text{–}CH_2OH \rightarrow CH_3CHO + H_2O \tag{1a}$$

$$2CH_3CHO \rightarrow CH_3COCOCH_3 + 2H^+ + 2e^- \tag{1b}$$

The cathodic polarization of Ag particles by electron transfer from organic radicals and reduction of Cu^{2+} on the surfaces of the Ag particles may accelerate reduction of Cu^{2+} in the presence of Ag particles. The activation polarization of the $Cu^{2+} + 2e^- \rightarrow Cu^0$ charge-transfer reaction and the diffusion polarization in the mass-transfer process may also participate in the enhancement of reduction of Cu^{2+} on Ag particles.

We found that no Cu/Ag alloys were formed in our conditions. One reason is that the reduction rate of Ag^+ is much faster than that of Cu^{2+} at 175 °C. If Cu^0 particles are formed, they are oxidized again by the following replacement reaction.

$$2Ag^+ + Cu^0 \rightarrow Cu^{2+} + 2Ag^0 \tag{2}$$

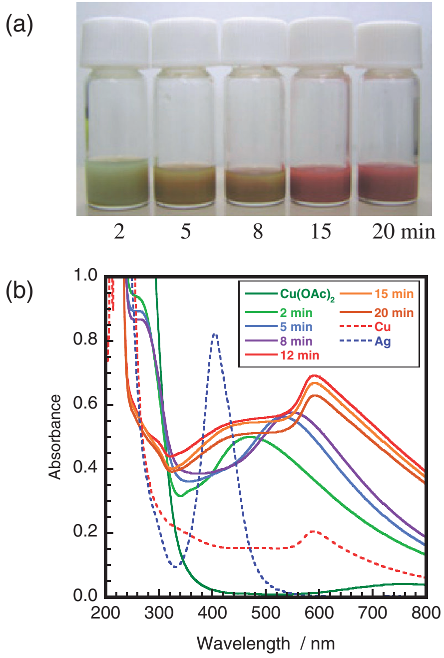

Figure 4. (a) Colors of solution at 2–20 min and (b) UV–vis spectra of $Cu(OAC)_2 \cdot H_2O$ solution, Ag@Cu nanoparticles obtained after heating for 2–20 min, and spherical Cu and Ag particles.

This is the other reason why no Cu/Ag alloys are formed in our conditions.

In summary, we succeeded in the preparation of Ag@Cu particles using a simple one-pot polyol reduction method. The thickness of Cu shells could be controlled by changing the reaction time.

We thank Mr. Takeshi Tanaka for his TEM–EDS measurements. This work was supported by the Joint Project of Chemical Synthesis Core Research Institutions, Grant-in-Aid for Scientific Research from the Japanese MEXT (Nos. 19033003 and 19310064), and Kyushu University G-COE program "Novel Carbon Resource Sciences."

References and Notes

1 J.-W. Hu, J.-F. Li, B. Ren, D.-Y. Wu, S.-G. Sun, Z.-Q. Tian, *J. Phys. Chem. C* **2007**, *111*, 1105; S. Deng, K. C. Pingali, D. A. Rockstraw, *IEEE Sens. J.* **2008**, *8*, 730; Y. Yang, J. Shi, G. Kawamura, M. Nogami, *Scr. Mater.* **2008**, *58*, 862.
2 K. J. Major, C. De, S. O. Obare, *Plasmonics* **2009**, *4*, 61.
3 M. Tsuji, N. Miyamae, S. Lim, K. Kimura, X. Zhang, S. Hikino, M. Nishio, *Cryst. Growth Des.* **2006**, *6*, 1801.
4 M. Tsuji, *Core–Shell Particles*, in *Shape and Structure Control of Metal Nano- and Fine-particles*, ed. by T. Yonezawa, CMC publishing, Tokyo **2009**, p. 166. (in Japanese).
5 M. Tsuji, S. Hikino, Y. Sano, M. Horigome, *Chem. Lett.* **2009**, *38*, 518.
6 M. Tsuji, S. Hikino, R. Tanabe, Y. Sano, *Chem. Lett.* **2009**, *38*, 860.
7 M. Cazayous, C. Langlois, T. Oikawa, C. Ricolleau, A. Sacuto, *Phys. Rev. B* **2006**, *73*, 113402.
8 T. Nakamura, Y. Tsukahara, T. Yamauchi, T. Sakata, H. Mori, Y. Wada, *Chem. Lett.* **2007**, *36*, 154.
9 M. Tsuji, S. Kumagae, M. Matsunaga, X. Tang, R. Tanabe, M. Ogino, to be published.
10 A. Henglein, M. Giersig, *J. Phys. Chem.* **1994**, *98*, 6931.
11 M. Tsuji, M. Hashimoto, Y. Nishizawa, M. Kubokawa, T. Tsuji, *Chem.—Eur. J.* **2005**, *11*, 440.